Published in: Clinical Cancer Research: Zeitschrift für Physikalische Chemie (1996), . Bd. 195, pp. S. 153-179
Status: Postprint (Author's version)

How Complex can be the Unimolecular Decomposition of a Simple Molecule?
The Case of Acetylene. An Electron Impact and PIPECO Investigation

By R. Locht[1] and Ch. Servais[2]

[1] *Départment de Chimie Générale et de Chimie Physique, Institut de Chimie, Bât. B6, Université de Liège, Sart-Tilman par B-4000 Liège 1, Belgium*
[2] *Institut d'Astrophysique, Bât. El, Université de Liège, Avenue de Cointe, 5, B-4000 Liège, Belgium*

Dedicated to Prof. Dr. H. Baumgärtel on the occasion of his 60th birthday

Abstract: The dissociative ionization of C_2H_2, C_2D_2 and C_2HD is presented in this work. Excepting the H_2^+ ion formation, all dissociation channels are thoroughly investigated by electron impact. The translational energy distribution as a function of the impinging electron energy and the appearance energy as a function of the translational energy are measured for all fragment ions. KE versus AE diagrams are obtained and the isotope effect is examined. All observed thresholds are analyzed in detail and dissociation mechanisms are proposed. For the C_2H^+ ion, the PIPECO technique has also been used. From these discussions the H-C_2H, HC≡CH and H-C_2 binding energy values are proposed, i.e. 5.33±0.23eV, 9.83±0.10eV and 5.44±0.40 eV respectively. The fragmentation paths leading to C^+, CH_2^+ and C_2^+ are discussed in terms of dissociation mechanisms involving the transient vinylidene structure of the molecular ion as an intermediate.

Keyword: Acetylene / Dissociation / Electroionization / Photoionization / Coincidence / Kinetic energy

Die dissoziative Ionisation von C_2H_2, C_2D_2 und C_2HD wird in dieser Arbeit vorgestellt. Sâmtliche der dissoziativen Zerfallskanäle, bis auf die H_2^+-Bildung, wurden mit Hilfe der Elektronenstoβionisation untersucht. Für sâmtliche Fragmentionen wurde die Verteilung der Translationsenergie als Funktion der Energie der auftreffenden Elektronen sowie die Auftrittspotentiale als Funktion der Translationsenergie gemessen. KE-AE-Diagramme werden ermittelt sowie Isotopeneffekte bestimmt. Die experimentellen Schwellenenergien werden im Detail analysiert, so daβ sich Dissoziationsmechanismen ableiten lassen. Zur Bestimmung der Eigenschaften des C_2H^+-Ions wurde die PEPICO-Technik verwendet. Aus den experimentellen Resultaten lassen sich die Bindungsenergien von H-C_2H, HC≡CH und H-C_2 ableiten, die 5,33±0,23 eV, 9,83±0,10 eV, 5,44±0,40 eV betragen. Die Bildung von C^+, CH_2^+ sowie C_2^+ wird mit Hilfe eines Dissoziationsmechanismus diskutiert, der eine transiente Vinyliden-Struktur des intermediären Molekülions beinhaltet.

1. INTRODUCTION

The chemical reaction and the chemical reactivity have certainly been among the major scientific concerns of Professor H. Baumgärtel. One of the priority axis of his own research and that of his successive students has been the investigation of the unimolecular decomposition of molecular ions by almost all existing techniques. Since more than fifteen years these investigations were extended to molecular clusters. He also pioneered the use of new light sources for ionization, e.g. synchrotron (DESY, BESSY) and laser radiation.

The present contribution to the 60th birthday of Professor H. Baumgärtel is in this research line and a symbol of our already more than fifteen years old but still strong collaboration.

The investigation of acetylene has first been motivated by the scarcity of the data related to its dissociative ionization. On the other hand, it looks a simple system including both π and σ bonding. Formally, this molecule is also isoelectronic with N_2, in which CH is the "separated atomic species" corresponding to the N atom. In the most recent past, the H-C_2H binding energy has been the subject of a long dispute in numerous papers [1]. The HC≡CH bond could be carefully investigated. Finally, rearrangement ions, e.g. CH_2^+, can be studied allowing us to examine the possible isomerisation of the acetylenic molecular ion into e.g. its vinylidenic isomer.

In the present contribution we gathered all the experimental material related to the dissociative ionization of this molecule obtained recently by electron impact and photoionization experiments.

Published in: Clinical Cancer Research: Zeitschrift für Physikalische Chemie (1996), . Bd. 195, pp. S. 153-179
Status: Postprint (Author's version)

2. EXPERIMENT

Two experimental techniques were used in this work: an electroionization experiment, already described in detail elsewhere [2] and a photoion-photoelectron coincidence spectrometer recently built and described in a forthcoming publication [3]. Only the most salient features of these setups will briefly be described below.

By the impact of energy controlled electrons the ions produced in a Nier-type ion source are allowed to drift out of the ion chamber, are fo-cussed on the ion source exit hole, energy analyzed by a retarding lens and mass selected in a quadrupole mass spectrometer. The detected ion current is continuously scanned as a function of either the electron energy at fixed retarding potential settings V_R or the retarding potential at fixed electron energy E_e. Both signals are electronically differentiated. Most of the experimental parameters are computer controlled.

In the photoion-photoelectron (PIPECO) experiment the gaseous sample is effusively introduced in an ion chamber. Perpendicular to the photoelectron-photoion optical axis, the light produced by a discharge lamp is introduced into the ion chamber through a capillary of 0.5 mm diameter. Photoions are extracted by a weak electric field (100 $mV \cdot cm^{-1}$) and are focussed on the entrance hole of a quadrupole mass spectrometer. Coaxially, in the opposite direction to the ions, photoelectrons are extracted and analyzed in a retarding field spectrometer with a differential output, as designed by Lindau *et al.* [4]. Both the photoion source and photoelectron spectrometer are surrounded by two μ-metal cylinders to cancel all external magnetic fields. A photoelectron energy resolution of 30 meV is obtained in coincidence conditions. Photoion kinetic energy distributions are measured by a retarding potential analyzer and a HWHM of 30 meV is obtained for translational energy distributions of molecular ions. The electron and ion detectors are 17-stage electron multipliers with 20 ns FWHM output pulses. The power supplies used to drive both the electron energy analyzer and the ion optics are programmable by IBM PC through an RS 232 I/O port.

The hardware and software for the data acquisition in time-of-flight (TOF), PIPECO-, photoion kinetic energy- and mass spectrum-measuring modes were developed and installed on a FPGA-based, home-made interface inserted in an IBM-PC slot. Additional external modules were built for TOF measurement and coincidence gates generation.

Both experiments are mounted in a vacuum vessel baked-out at about 250 °C to obtain an ultimate vacuum lower than 10^{-8} Torr. For the electron impact experiment a sample pressure of 10^{-6} Torr is used whereas in the photoionization experiment a sample pressure of $2x10^{-5}$ Torr is used for photoelectron spectra and translational energy distribution measurements. For TOF- and coincidence measurements a pressure lower than $2x10^{-6}$ Torr of acetylene is used for better coincidence statistics and to avoid ion molecule reactions.

The C_2H_2 sample, of 99.997% purity and mixed with 1% acetone in a high pressure cylinder, is used without further purification. Samples of 1 liter at 1 atm of C_2D_2 and C_2DH are of 99 and 93 at % purity respectively and are exempt from acetone.

The maximum of the molecular ions translational energy distribution is used as the zero-energy calibration point for the kinetic energy scale. This reference is continuously recorded during the measurement of the ionization efficiency curves of the fragment ions by electron impact. In the photoionization experiment the same calibration point has been maintained.

In the electron impact experiment, the electron energy scale is calibrated by using the production of N_2^+ and N^+ from N_2 at 15.581 eV and 24.294 eV respectively [5]. When *m*/*e* interference exists, e.g. CD^+ or CH_2^+ and N^+ the ionization energy of Ne at 21.564 eV [6] is used. In the PIPECO-experiment the photoelectron energy scale is calibrated by using the adiabatic ionization energy of C_2H_2 in the $X^2\Pi_u$ state at 11.403 eV [7].

All the results and measurements presented in the following sections are the result of several independent experiments performed to ensure reproducibility and to increase the signal-to-noise ratio by summation of the signals. This allows us also to estimate correctly the error on the measurements. In the diagrams displayed in this work, straight lines are fit to the data by linear regression and the error on both the slope and extrapolation are calculated [8].

In the PIPECO-measurements, the TOF-distribution curves and the coincidence spectra are systematically smoothed to increase the signal-to-noise ratio. The smoothing procedure uses the Fourier

transform incorporating appropriate filtering operators.

3. EXPERIMENTAL RESULTS

Excepting the H_2^+ ion production, all the dissociative ionization channels occurring in C_2H_2 have been investigated. For sake of clarity in the presentation of the experimental results and their discussion in the following sections, the ionization channels were classified by (i) the H^+ and C_2H^+ formation as leading to the estimation of the H-C_2H binding energy, (ii) the CH^+ formation giving access to the HC≡CH binding energy measurement and (iii) the production of C^+, C_2^+ and CH_2^+ which involves the vinylidenic ion as an intermediate.

3.1 The $H^+(D^+)$ and $C_2H^+(C_2D^+)$ formation

The $H^+(D^+)$ dissociation channel has been investigated in C_2H_2 and C_2D_2 for two reasons: (i) to avoid any confusion of H^+ with other proton sources, e.g. H_2O (from the background), acetone (present in the sample) and/or H_2 produced by the possible thermolysis of hydrocarbons on the electron emitting filament, (ii) to investigate the isotope effect on the slope of the straight line in the kinetic energy (KE) versus appearance energy (AE) diagram. This isotope effect gives valuable informations on the dynamics of the considered dissociation channel.

The proton (deuteron) ion energy distribution has been measured for electron energies ranging from 22-99 eV. The first differentiated ionization efficiency curves of H^+ (D^+) have been recorded between 15-45 eV electron energy for retarding potential settings increasing from 0.0-10.0 V. The KE versus AE plot resulting from these measurements is shown in Fig. 1 for H^+.

Fig. 1: *The KE versus AE diagram for H^+/C_2H_2 in the 17-42 eV electron energy range. The encircled numbers are used in the discussion (see text). The length of the error bars represent the standard deviation.*

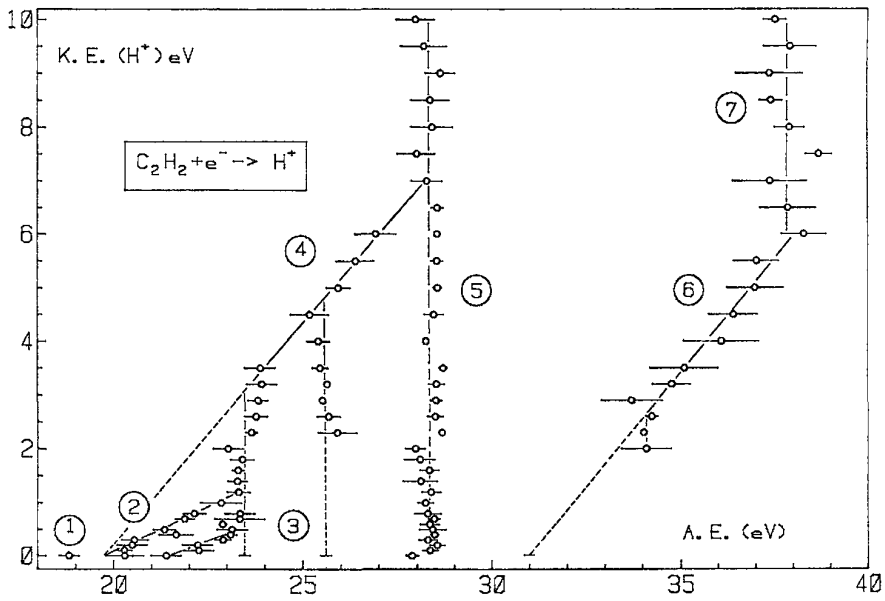

For 0.0 V retarding potential, this diagram clearly shows four threshold energies, i.e. at 18.8±0.2eV, 20.3±0.4eV, 21.4±0.4eV and at 27.8± 0.2 eV. The drawn straight lines 2-7 are the result of linear regressions fit to the experimental data and four vertical lines are observed, i.e. at 23.5±0.3 eV, 25.6±0.2 eV, 28.4±0.2 eV and at 37.4±0.5 eV. Fig. 2 shows the result of the same measurements on D^+ from C_2D_2 in a narrow retarding potential range of 0.0-1.6 V. In this diagram the results on H^+ from C_2H_2 are inserted for comparison. Appearance energies are observed at 19.3±0.1 eV, 20.5±0.2 and 21.4±0.2eV. A vertical line is starting at 28.3±0.2 eV up from V_R = 0.3 V.

The ion translational energy distribution and the ionization efficiency of C_2H^+ (C_2D^+) have been

Published in: Clinical Cancer Research: Zeitschrift für Physikalische Chemie (1996), . Bd. 195, pp. S. 153-179
Status: Postprint (Author's version)

investigated. The KE distribution is quite similar to that of the molecular ion and the ionization efficiency could only be recorded for weak (<50 mV) retarding potential settings (see Fig. 3). This result is expected, the C_2H^+ ion carrying 1/26 part of the total excess kinetic energy, on the base of the momentum conservation law. Clearly two onset energies are observed, i.e. at 17.30±0.08 eV and 18.27±0.11 eV for C_2H^+ and at 17.38±0.11 eV and 18.45±0.26 eV for C_2D^+.

The C_2H^+ dissociation is the only channel which could be investigated by PIPECO. Though observed in the mass spectrum of C_2H_2 recorded at 54.8 nm, the C_2^+ ion could not be measured within a reasonable time. Fig. 4 shows the translational energy distribution observed at 58.4 nm and is compared to $C_2H_2^+$ in the same figure. No significant differences have to be mentioned. Closely related to the KE carried away by the ion, the maximum of the TOF-distribution of C_2H^+ has been measured at 33 μs as shown in Fig. 5.

Fig. 2: *The KE versus AE diagram for D^+/C_2D_2 in the 0.0-1.2 V retarding potential range (full dots). The encircled numbers refer to the same processes observed for H^+/C_2H_2 (open circles). The length of the error bars is equal to the standard deviation.*

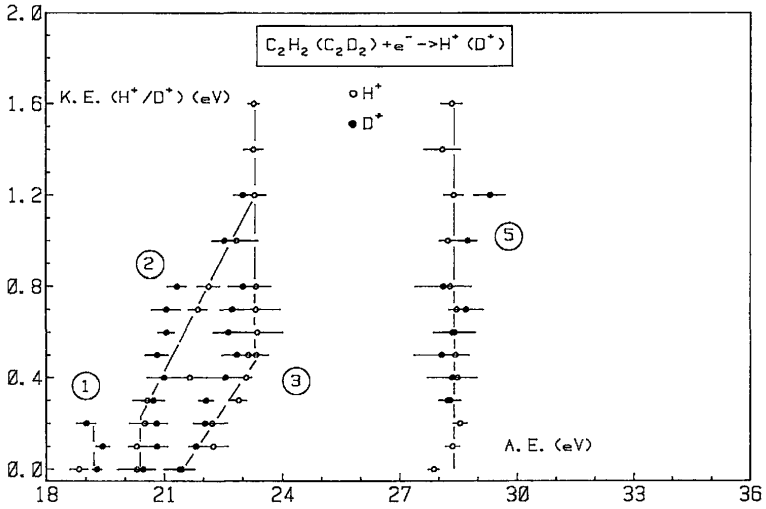

Fig. 3: *The first differentiated ionization efficiency curve of C_2H^+/C_2H_2 and C_2D^+/C_2D_2 as observed without applying a retarding field. The vertical bars locate the average onset energies.*

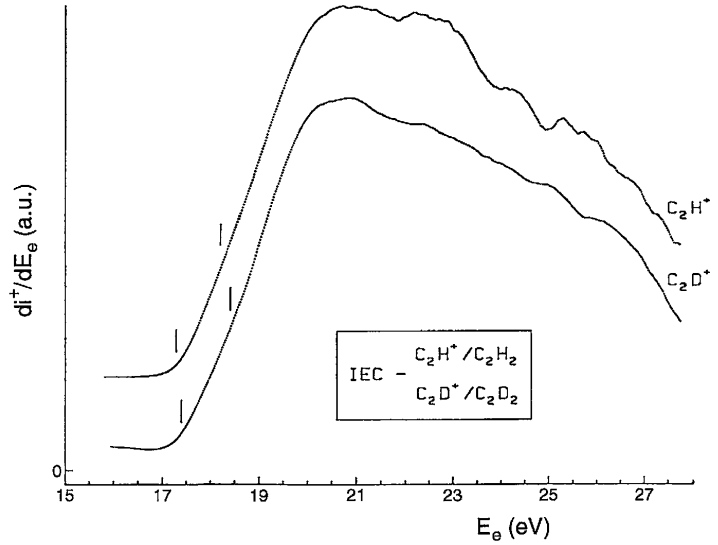

Published in: Clinical Cancer Research: Zeitschrift für Physikalische Chemie (1996), . Bd. 195, pp. S. 153-179
Status: Postprint (Author's version)

Fig. 4: *The first differentiated retarding potential curves of the C_2H^+ (full line) and $C_2H_2^+$ (dotted line) ions recorded at 58.4 nm.*

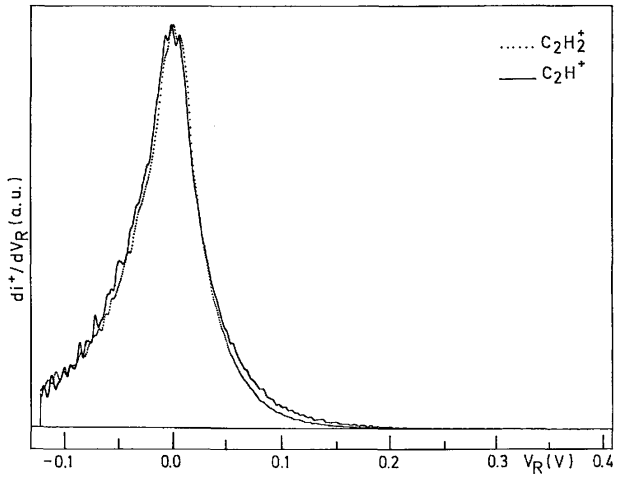

Fig. 5: *TOF-spectrum of $C_2H_2^+$ and C_2H^+ ions from C_2H_2 in coincidence with 2.5 eV photoelectrons (corresponding to the $B^2\sum_u^+$ state of $C_2H_2^+$). The signal is filtered by fast Fourier transform with a cos^4 operator.*

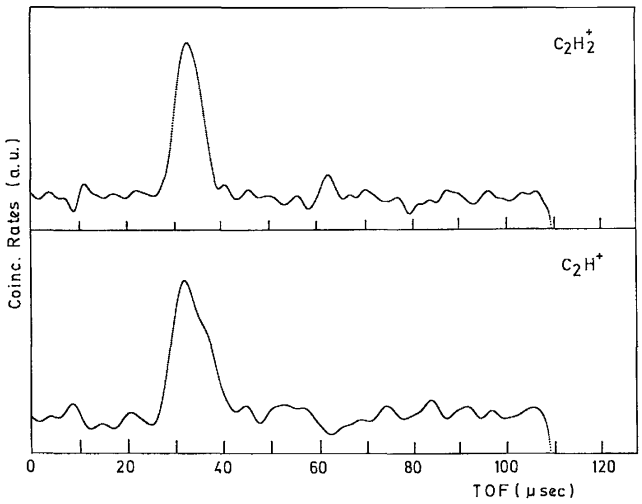

The maximum of the $C_2H_2^+$-TOF distribution occurs at 33 μs, confirming the translational energy displayed in Fig. 6 for TOF = 33 μs, together with the photoelectron spectrum of C_2H_2 in the range of 16.2—20.2 eV ionization energy. Both coincidence spectra show structures strongly correlated with the photoelectron spectrum. The vibrational fine structure is clearly visible. It is important to mention that these spectra were recorded at low sample pressure, i.e. below 10^{-6} Torr. At higher pressures the mass spectrum shows the occurrence of m/e = 50, assigned to $C_4H_2^+$ or $(C_2H)_2^+$ dimeric ions. At these pressures, C_2H^+ has to be suspected to arise from these species.

3.2 The $CH^+(CD^+)$ formation

Typical CH^+ ion kinetic energy distributions, as observed close to threshold, are shown in Fig. 7. At the threshold of CH^+ formation the maximum of the distribution is measured at 0.025 ±0.008 eV and the FWHM is 120 meV. Above 21 eV electron energy and up to 99 eV new contributions are detected.

Published in: Clinical Cancer Research: Zeitschrift für Physikalische Chemie (1996), . Bd. 195, pp. S. 153-179
Status: Postprint (Author's version)

Fig. 6: *The photoelectron spectrum (a) of C_2H_2 as measured under coincidence conditions in the 16.2-20.2 eV ionization energy range. The assignment of the two vibronic bands are indicated. Photoion-photoelectron coincidence spectra of (b) C_2H^+ and (c) $C_2H_2^+$ are shown in the corresponding energy range. The latter signals are filtered by fast Fourier transform. The arrow and dashed area show the onset for appearance of C_2H^+ and the signal vanishing of $C_2H_2^+$ and the associated uncertainty respectively.*

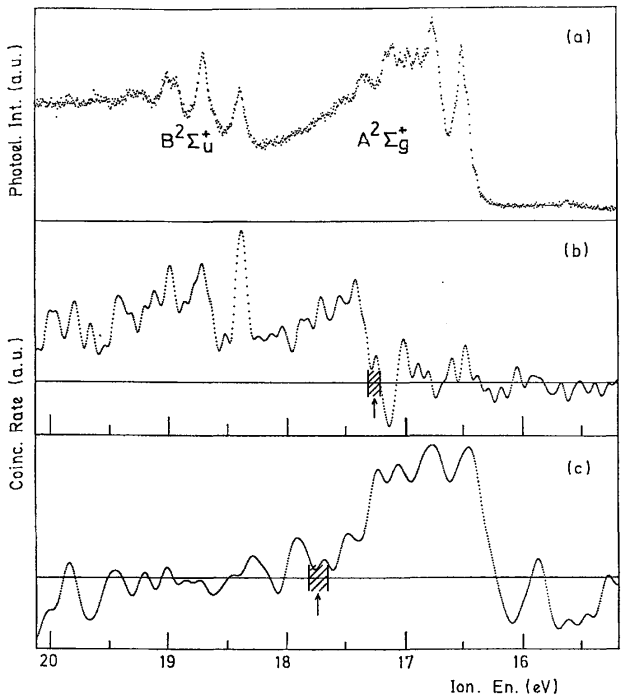

The first differentiated ionization efficiency curves of CH^+ from C_2H_2 have been recorded for increasing retarding potential settings. In the high electron energy range of the ionization efficiency an important contribution originates from doubly ionized C_2H_2 detected at *m/2e* = 13. The $C_2H|^+$ production has been studied earlier [1]. The KE versus AE diagram obtained for CH^+ is displayed in Fig. 8 and shows twelve processes. Four onsets are measured when no retarding field is applied, i.e. at 20.83±0.05 eV, 21.84±0.04 eV, 24.9±0.03 eV and 33.8±0.1 eV. This latter onset observed in the interval V_R = 0.0-0.1 *V* is ascribed to $C_2H_2^{2+}$ for which the lowest onset energy is at 32.2±0.2 eV and the second ionization energy (observed here) at 33.5±0.1 eV, as measured in C_2HD [1].

The same measurements have been performed on CD^+ from C_2D_2 and the results for V_R = 0.0-1.4 V are shown in the KE versus AE diagram in Fig. 9. Dramatic isotope effects are observed and the data related to CH^+ are inserted for comparison. For CD^+ onset energies are determined at 20.61 ±0.07 eV, 21.26±0.08 eV and 21.84±0.07 eV in the electron energy range of 20-28 eV.

3.3 The C^+, CH_2^+ and C_2^+ formation

The C^+, C_2^+ and CH_2^+ dissociation channels have been studied by measuring both the translational energy distribution of these ions as a function of the electron energy E_e and the first derivative of the ionization efficiency as a function of the retarding potential V_R. The results obtained by this way are presented in the KE versus AE diagrams corresponding to these fragment ions. Fig. 10 shows such a plot related to C^+ where clearly six processes are observed. For V_R = 0.0 *V* threshold energies at 21.6±0.30 eV, 22.24± 0.20 eV, 23.6±0.2 eV and at 26.5±0.1 eV are measured in the first differentiated ionization efficiency curve.

For the C_2^+ ion the translational energy distribution is similar to the thermal distribution observed for the molecular ion. This observation is expected, the C_2^+ ion carrying only 2/26 part of the total excess translational energy involved in the decomposition reaction. Moreover, its ionization efficiency curve could only be observed for retarding potential settings V_R < 0.05 *V*. Threshold energies were measured at 18.44±0.07 eV, 19.58± 0.14 eV and 23.00±0.11 eV successively in C_2H_2 and at 18.5±0.2eV, 19.5±0.3 eV and at 23.12±0.12 eV in C_2D_2.

Published in: Clinical Cancer Research: Zeitschrift für Physikalische Chemie (1996), . Bd. 195, pp. S. 153-179
Status: Postprint (Author's version)

In spite of the precautions taken for keeping the background mass spectrum as low as possible, above the appearance energy of N^+/N_2, at 24.293 eV [5], this species buries the CH_2^+ signal. Therefore the KE distribution and the appearance energy data are not considered above the 24.3 eV energy limit. The data thus obtained are displayed in the KE versus AE plot shown in Fig. 11 where clearly two CH_2^+ producing processes are detected below 24.3 eV, i.e. 19.74±0.12eV and 21.10±0.20eV. Together with the results related to CH_2^+, those corresponding to N^+/N_2, investigated earlier [9], have been included. The excellent agreement between the two measurements convincingly confirms the detection of N^+ instead of CH_2^+ above 24.3 eV.

Fig. 7: *The first differentiated retarding potential curves of CH^+/C_2H_2 close below and above the appearance energy of this ion.*

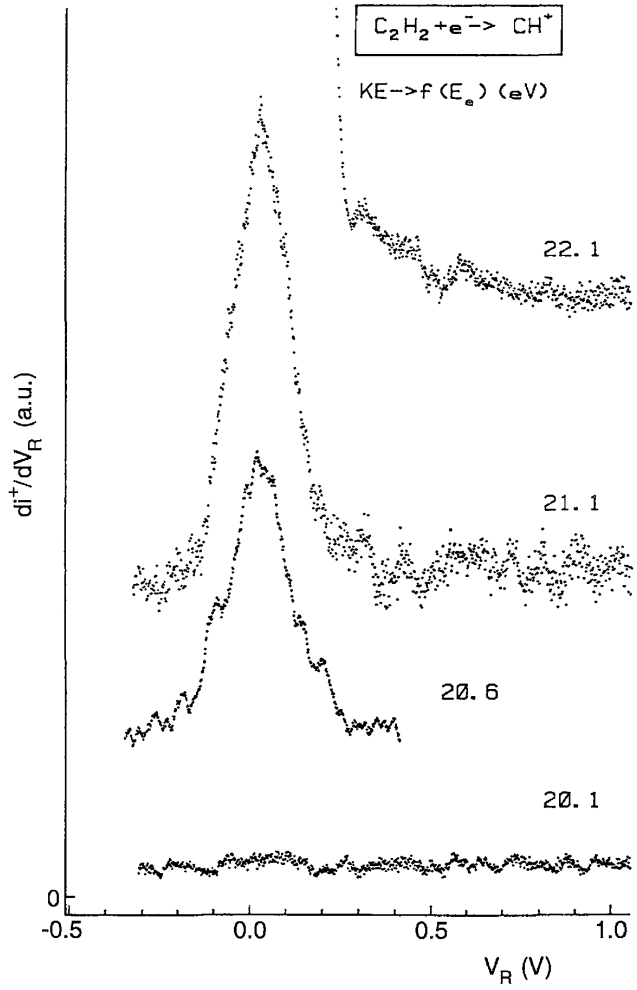

4. DISCUSSION

For the easiness and clarity in the following discussion, all the data used to calculate threshold energies for dissociative ionization processes giving rise to the ions to be considered in this work are gathered in Table 1.

The C_2H_2 molecule belongs to the $D_{\infty h}$ symmetry group and the electronic configuration of the ground vibronic state $X^1\sum_g^+$ is described by

$$(1\sigma_g)^2(1\sigma_u)^2(2\sigma_g)^2(2\sigma_u)^2(3\sigma_g)^2(1\pi_u)^4.$$

Three ionic states are observed in the He(I)-photoelectron spectrum. The adiabatic ionization energies are measured at 11.403 eV ($X^2\Pi_u$), 16.297 eV ($A^2\Sigma_g^+/A^2A_g$) and 18.391 eV ($B^2\Sigma_u^+$) [7]. The He(II)-photoelectron spectrum shows two more bands with a vertical ionization energy at 23.6 eV and at 27.6 eV successively [10]. The threshold photoelectron spectrum, obtained with synchrotron radiation [11], shows the existence of Rydberg

states autoionizing to $C_2H_2^+$ ($X^+\Pi_u$) state and a structureless autoionizing state starting at 21.0 eV.

Fig. 8: *The KE versus AE diagram of CH^+/C_2H_2 in the 20-40 eV electron energy range. The encircled numbers are used for the discussion (see text). The length of the error bars is given by the standard deviation.*

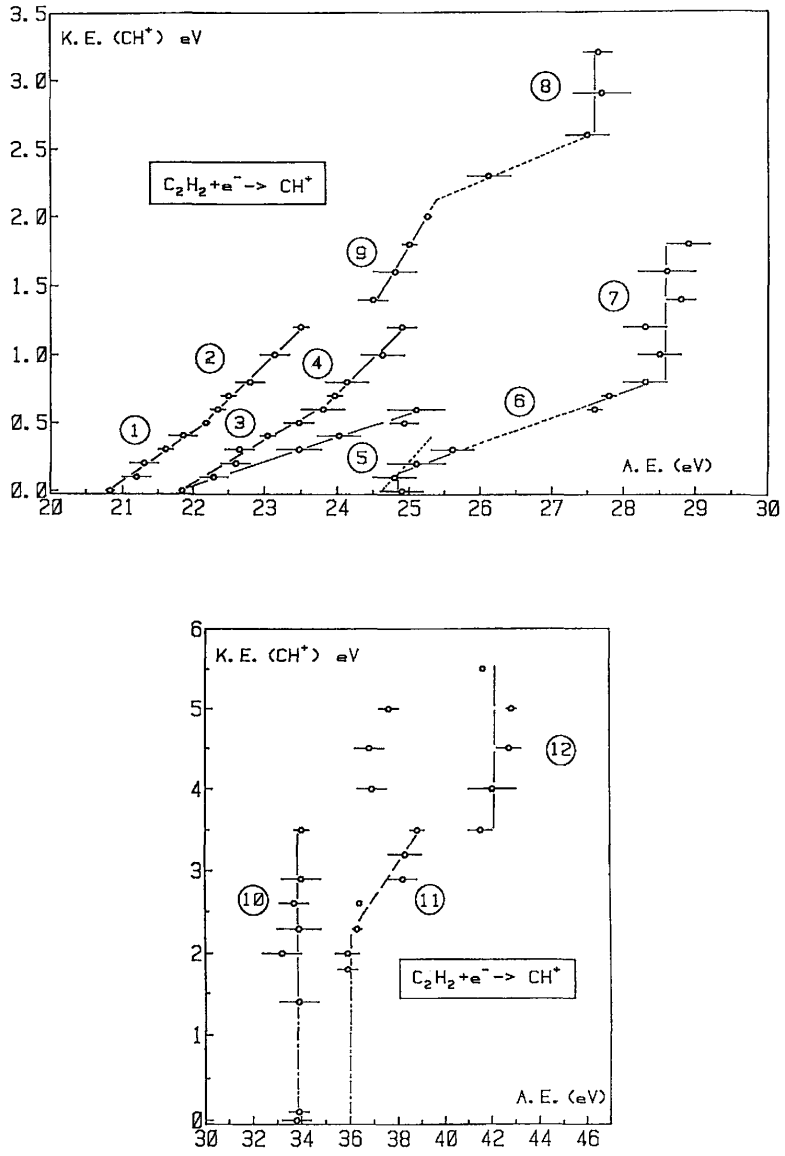

4.1 The $H^+(D^+)$ and $C_2H^+(C_2D^+)$ dissociation channels

4.1.1

The lowest onset for H^+ production from C_2H_2 is measured at 18.83±0.23 eV, whereas D^+ is observed at 19.2±0.2eV. The former ion carries no translational energy, the latter is produced with 0.2 eV KE at threshold (see Fig. 2). Therefore, the $AE(D^+)_{KE=0.0}$= 19.03±0.2 eV. The KE versus AE dependence of line (1) in Figs. 1 and 2 and the agreement within experimental error between both onsets warranties the proton is produced from C_2H_2 only. No other source has to be suspected at this onset.

The only electron impact determination is from Kusch *et al.* [18] reporting the lowest threshold of H^+ at 21.7 ±1.0 eV. More recently Shiromura *et al.* [19] measured the same onset at 19.35±0.05 eV by photoionization

using synchrotron radiation. The calculation of the lowest appearance energy for the reaction

$$C_2H_2 + e^- \rightarrow C_2H_2^+(B^2\Sigma_u^+) \xrightarrow[A^2\Sigma_g^+]{\text{prediss}} C_2H(X^2\Sigma^+) + H^+(^1S_g) + 2e^- \qquad (1)$$

Fig. 9: *The KE versus AE diagram of CD^+/C_2D_2 (full lines and full circles) restricted to the 0.0-1.5 eV translational energy range. For comparison the data related to CH^+/C_2H_2 (dotted lines and empty circles) are introduced. Encircled numbers are used in the discussion (see text).*

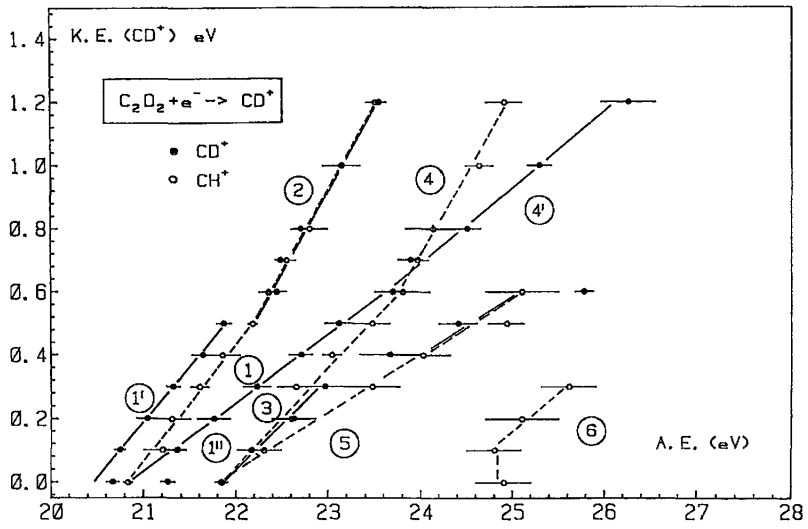

needs the value of the dissociation energy D(H-C_2H). The present work provides (i) the translational energy at threshold, i.e. KE = 0.0 eV and (ii) the corresponding onset being 18.9±0.2 eV, i.e. the average of the appearance energy of H^+ and D^+. If the radical C_2H is supposed to be *formed without internal energy* a dissociation energy *D(H-C_2H) = 5.33±0.20 eV* is derived (for the data used, see Table 1). The comparison of this value of the binding energy with that obtained by studying the counterpart reaction, i.e. $C_2H_2^+ \rightarrow C_2H^+ + H$ and with previous determinations, will be presented in section 4.1.2.

Fig. 10: *The KE versus AE diagram of C^+/C_2H_2 in the 20—37 eV electron energy range. Encircled numbers are used in the discussion (see text).*

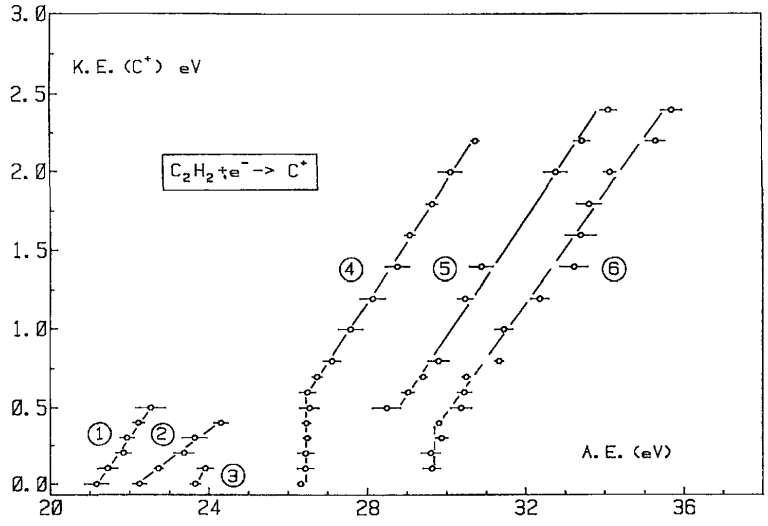

Published in: Clinical Cancer Research: Zeitschrift für Physikalische Chemie (1996), . Bd. 195, pp. S. 153-179
Status: Postprint (Author's version)

Fig. 11: *The KE versus AE diagram of CH_2^+/C_2H_2 in the 18-29 eV electron energy range. Encircled numbers are used for the discussion (see text). The dashed straight line has a slope of 12/26 = 0.46. The full circles refer to the data on N^+/N_2 as measured in an earlier work [9].*

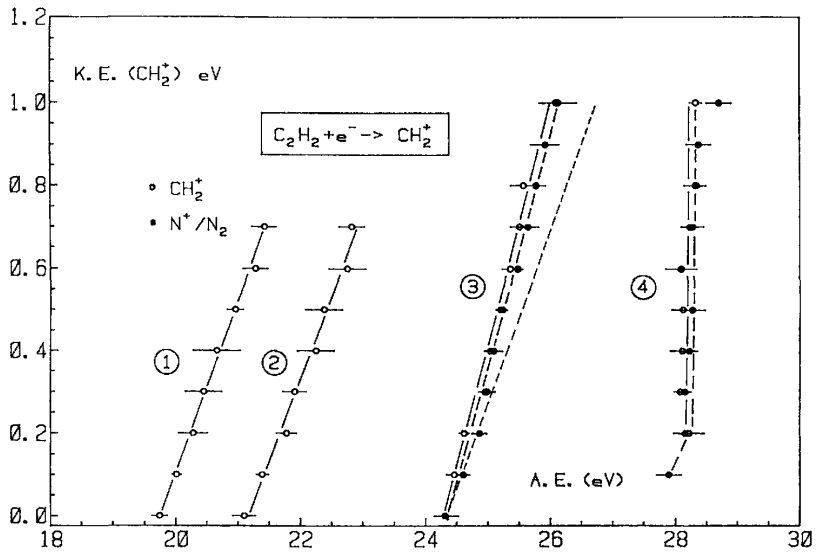

Table 1: *Dissociation (D), ionization (IE), excitation (EE) energies and electron affinities (EA) (eV) of C_2H_2, C_2H, CH_2, C_2, H_2, CH, C and H used in this work*[a].

$D(HC_2\text{-}H) = 5.33\pm0.20$[b]	EE(H, n = 2) = 10.210
$D(HO{\equiv}CH) = 9.83\pm0.10$[b]	$EE(C,{}^1D) = 1.264$
$D(C_2\text{-}H) = 4.85\pm0.31$[c]	$(C,{}^1S) = 2.684$
$D(HC\text{-}H) \geq 4.33$ [d]	$EE(C^+,{}^4P) = 5.331$
$D(C{\equiv}C) = 6.21$	$(C^+,{}^2D) = 9.290$
D(C-H) = 3.465[e]	$EE(CH,a^4\Sigma^-) = 0.724$
D(H-H) = 4.476	$(A^2\Delta) = 2.875$[e]
IE(H) = 13.598[f]	$(B^2\Sigma^-) = 3.229$
(C) = 11.264[f]	$(C^2\Sigma^+) = 3.943$
(CH) = 10.64[e]	$EE(CH^+,a^3\Pi) = 1.141$
$(C_2) = 12.15$[e]	$(A^1\Pi) = 2.898$
$(CH_2) = 10.396$[d]	$(b^3\Sigma^-) = 4.736$[e]
EA(H) = 0.754[g]	$(B^1\Delta) = 6.513$
$(C_2H) = 2.969\pm0.010$[h]	$EE(C_2^+,D^1\Sigma_u^+) = 5.361$[e]
	$EE(CH_2,a^1A_1) = 0.394$
	$(b^1B_1) = 1.270$
	$(B^3\Sigma_u^-) = 8.757$

[a] 1 eV = 23.060 kcal mol^{-1} = 8065.73 cm^{-1}.
[b] As measured in this work.
[c] Ref. [12];[d] Ref. [13];[e] Ref. [14];[f] Ref. [6];[g] Ref. [15];[h] Ref. [16];[i] Ref. [17].

The vibronic state of both fragments in reaction 1 correlate with a $C_2H_2^+$ ($^2\Sigma^+$) state. The energy level of 18.9 eV, together with this symmetry, strongly suggests the $C_2H_2^+$ ($A^2\Sigma_g^+$) being a good candidate to be involved in process 1. On the other hand, the $C_2H_2^+$ ($B^2\Sigma_u^+$) is populated by Franck-Condon transition in this energy range (see Fig. 6a). The H^+ (D^+) ions would be produced by predissociation of the $B^2\Sigma_u^+$ state through the $A^2\Sigma_g^+$ state. The C_2D_2 photoelectron spectrum shows an unusually strong isotope effect on the vibrational structure. This could explain the drastic differences observed for H^+ and D^+ production at their lowest onset.

The second onset for H^+ is observed at 20.3 ±0.4 eV. It is the starting point of straight line (2) in Fig. 1. This linear regression fits the data with a correlation coefficient of 0.994, the slope is 0.34±0.01 and the

extrapolation is 19.82±0.08 eV. For D^+ the corresponding onset is 20.4±0.12 with a slope of 0.9 ±0.1 with a correlation coefficient of 0.86. The slope expected from the momentum conservation law is given by the ratios 25/26 = 0.96 and 26/28 = 0.93 for H^+/C_2H_2 and D^+/C_2D_2 respectively. The experimental and expected slopes agree fairly well in C_2D_2, whereas in C_2H_2 the discrepancy is significant. It indicates the partial (about 60%) excess energy conversion into internal energy of the polyatomic fragment C_2H [20]. The large difference in the dynamics of the reaction has very likely to be correlated with the strongly perturbed vibrational structure by isotopic substitution observed in C_2D_2.

The excess energy of 20.3(±0.3)-18.9(±0.2) = 1.4+0.5 eV has to be ascribed to vibronic excitation of the C_2H radical. Several quantum mechanical [21-23] and spectroscopic [24-26] investigations of this radical have been reported. The lowest excited state should level at about 0.5 eV above the ground state and should have the $^2\sum$ multiplicity and symmetry. Though the discrepancy between this experiment and theoretical predictions, it could be suggested that at 20.1 eV the reaction

$$C_2H_2^{+*} \rightarrow C_2H\ (A^2\Pi) + H^+\ (^1S_g) \qquad (2)$$

takes place, where the C_2H radical would carry a certain amount of internal energy. The H^+ (D^+) production very likely runs over a predissociation mechanism ascribed to the coupling of the B^2A_1, A^2A_1 and X^2A_1 states of $C_2H_2^+$ in the C_{2h} configuration [7]. This would also be the origin of the reversed isotope effect observed on the slopes of the straight lines.

The straight line (3) in Figs. 1 and 2 gives threshold energies at 21.4±0.3 eV and 21.46±0.22 eV for KE = 0.0 eV protons and deuterons respectively. The energy difference of 21.4(±0.3)-18.9(±0.2) = 2.5±0.5 eV is still too low to be assigned to the dissociation of the H-C_2 bond (see Table 1). It is also difficult to interpret these onsets because of lack of spectroscopic data related to C_2H. UV bands assigned to Σ-Σ transitions at 3405 Å have been reported [27]. Around 36000 cm^{-1} emission bands were observed and tentatively ascribed to Π-Σ transitions [26].

However, it is established that in the threshold photoelectron spectrum of C_2H_2 [11] a Rydberg state starts at 21.5 eV. Therefore, it could be proposed that the above mentioned processes should run over this autoionizing state giving rise to dissociative ionization.

Between 23 and 27 eV the KE versus AE diagram unequivocally shows two processes, i.e. at 23.5±0.3 eV and at 25.6±0.2eV, converging to the same limit. The linear regression provides a limit at KE(H^+) = 0.0 eV of 19.6±0.2 eV and a slope of 0.86±0.02. The phenomena observed at these energies have to run over ionic hypersurfaces of $C_2H_2^+$ identified as Σ^+ states in the He(II)- [28], TPES- [11] and X-ray photoelectron spectra [29]. These Σ^+ states are described [30] as repulsive in the H-C_2H reaction coordinate in the Franck-Condon region and will provide protons carrying large amounts of translational energy.

The results of the foregoing discussion have been schematically represented in a two dimensional potential energy diagram displayed in Fig. 12 for the H-C_2H reaction coordinate.

The vertical line (5) reveals high energy protons produced both by C_2H_2 and by acetone present in the sample. Fig. 2 related to C_2D_2 (acetone-free) disentangles the part coming from acetylene and is limited to the 0.0-1.2 eV kinetic energy range. For these protons, at the threshold measured at 28.3±0.2 eV the energy balance based on these data provides an $AE_{KE=0.0}$ (D^+) = 27.0±0.2 eV and should correspond very likely to the reaction

$$C_2H_2 + e^- \rightarrow C_2H_2^+\ (^2\Sigma^+) \rightarrow CH\ (X^2\Sigma) + C\ (^3P) + H^+\ (^1S_g) + 2e^- \qquad (3)$$

which should run over repulsive $^2\Sigma^+$ hypersurfaces [30].

After an energy gap of 4 eV, several processes are observed between 34 and 40 eV. The vertical line at 34.1 ±0.4 eV and the straight line extending up to 37.4±0.5 eV should correspond to the decomposition of the doubly ionized molecular ion by "Coulomb explosion". Double ionization energies of C_2H_2 were determined experimentally by several methods [1, 31], i.e. at 34.6±0.4 eV [1] and at 37.9±0.4 eV [31]. The latter onset being not detected in the $C_2H_2^{2+}$ ionization efficiency, this should indicate that this state is dissociative in the Franck-Condon region. The proton producing reaction should be

Published in: Clinical Cancer Research: Zeitschrift für Physikalische Chemie (1996), . Bd. 195, pp. S. 153-179
Status: Postprint (Author's version)

$$C_2H_2 + e^- \rightarrow C_2H_2^{2+} (^3\Pi/^3\Sigma^-) \rightarrow C_2H^+ (X^3\Pi/A^3\Sigma^-) + H^+ (^1S_g) + 3e^-. \quad (4)$$

Fig. 12: *Tentative schematic potential energy diagrams of $C_2H_2^+$ along the H-C_2H and the HC≡CH reaction coordinates. The areas shaded by horizontal lines define the well depth observed in the He(I) photoelectron spectrum. Dashed lines locate the experimental data and the results from the discussion about H^+, C_2H^+ and CH^+ fragments production.*

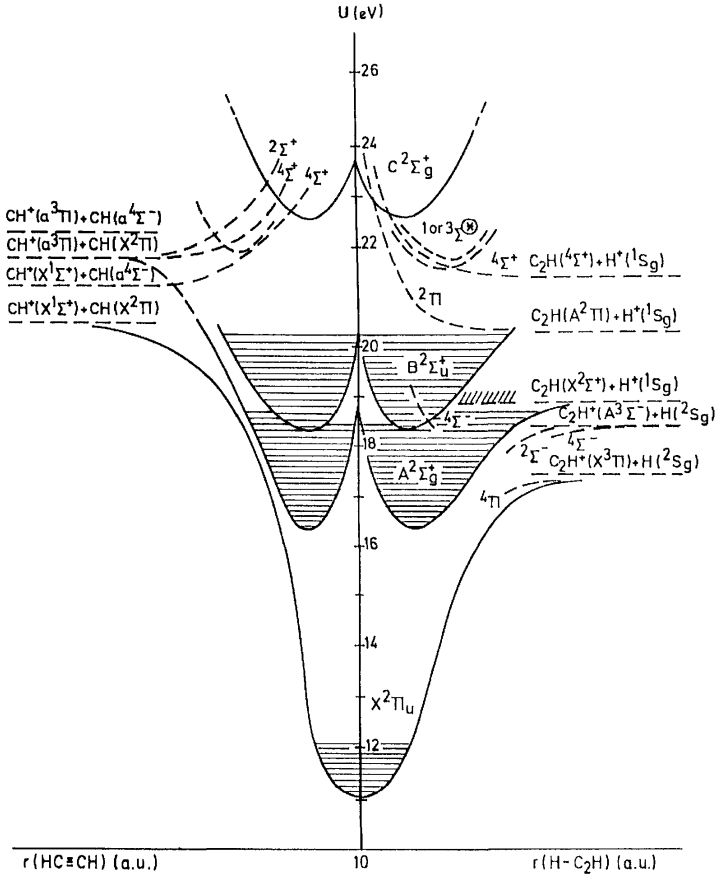

From an obvious energy balance, process (7) in Fig. 1 at 37.4±0.4 eV should involve superexcited states of $C_2H_2^+$ lying in the double ionization continuum.

4.1.2

As mentioned in section 3, the C_2H^+ ion could only be observed when no retarding potential is applied. This means that the ion carries less than 10 meV translational energy, i.e. 260 meV in terms of total translational energy. This is shown to be the case also with 21.22 eV photons (see Fig. 4).

The first observed onset for C_2H^+ and C_2D^+ is measured at 17.30±0.08 eV and 17.38±0.11 eV respectively (see Fig. 3). This is in very good agreement with most of the earlier electron impact and mass spectrometric photoionization experiments reported up-to-date [1]. However, Hayaishi *et al.* [32] and Ono and Ng [33] mention the lowest appearance energy to be 16.8±0.1 eV and 16.79±0.03 eV respectively. Recently ZEKE-PIPECO [34] and threshold PEPICO [35] works agree by measuring an onset at 17.36±0.01 eV and 17.44±0.01 eV. The second onset determined in this work, i.e. at 18.27±0.10 eV and 18.45±0.26 eV in C_2H_2 and C_2D_2 respectively, has never been reported earlier.

Concerning the first onset of C_2H^+ at 16.8 eV, it has to be pointed out that if there is good agreement for

the energy, large discrepancies for the relative cross section have to be mentioned. Relative intensity differences of one order of magnitude are observed. In their electron impact work Plessis and Marmet [36] had to amplify the C_2H^+ signal by 5000 to observe the onset at 16.7 eV. The main difference between these experiments [32, 33, 36] is the sample pressure. As mentioned in section 2, the present measurements were performed below 10^{-6} Torn In these conditions the $C_4H_2^+$ signal at *m/e* = 50 is negligible. The present electron impact experiments are also carried out in these conditions. The $C_4H_2^+$ has to be suspected as the source of C_2H^+ ions below 17.3 eV.

The lowest energetic process producing C_2H^+ and H in their ground state through the dissociative ionization reaction of C_2H_2 should be

$$C_2H_2 + e^-(h\nu) \rightarrow C_2H_2^+(A^2A_g) \xrightarrow[x^2\Pi]{\text{prediss}} C_2H^+(X^3\Pi) + H(^2S_g) + (2)e^- \quad (5)$$

The calculation of the appearance energy of C_2H^+ through reaction 5 would need (i) the H-C_2H binding energy and (ii) the adiabatic ionization energy of the C_2H radical. The translational energy involved in the process is less than 260 meV, as deduced from direct kinetic energy measurements. Supposing C_2H^+ being formed **without internal energy** and using the experimental value of IE(C_2H) = 11.6±0.5eV [37] and the binding energy D(H-C_2H) = 5.33±0.2eV proposed in this work (see section 4.1.1), an onset of 16.9 ±0.7 eV is calculated for process 5. This result is in very good agreement with the lowest and unreliable appearance energy obtained by photoionization measurements. However, considering the error limits, all the results are included in the 16.2—17.6 eV energy range.

Both quantities, i.e. IE(C_2H) and D(H-C_2H) are questionable. The latter has been discussed abundantly in the literature and ranges 5.0 < D(H-C_2H) ≤ 5.79 eV as determined by thermodynamic cycles [16, 38], proton transfer [39, 40], dissociative ionization [32, 33], and spectroscopy [41-43]. One of the most reliable value is obtained by negative ion electron detachment spectroscopy [16], i.e. 5.69±0.03 eV. Using this value and IE(C_2H) = 11.6±0.5 eV, an appearance energy of 17.29±0.53 eV is calculated and in excellent agreement with the result of the present work.

To make sure that the process measured at 17.3 eV has to be ascribed only to the decomposition of $C_2H_2^+$, the PIPECO spectrum has been measured and is shown in Fig. 6b. The onset for C_2H^+ unequivocally lies at 17.35±0.04 eV, i.e. at the point where the vibrational structure of the A^2A_g (or $A^2\Sigma_g^+$ in $D_{\infty h}$ symmetry) of $C_2H_2^+$ is broadened and disappears (see Fig. 6a). This latter observation is a witness to the predissociation of the A^2A_g state. On the other hand, Fig. 6c shows that the molecular ion does not survive to dissociative ionization above 17.7 eV. Finally, the present experiment being performed with He(I) radiation, the contribution of autoionization could almost be excluded. The result of the present work is in excellent agreement with the ZEKE-PEPICO [34] and threshold PEPICO [35] works. In the latter experiments, autoionization phenomena could participate to the dissociative ionization. Furthermore, it has been shown experimentally [44] that no ion-pair producing process occurs at this energy. Both the reactions

$$C_2H_2 + e^- \rightarrow C_2H^+ (C_2H^-) + H^- (H^+) + e^-$$

have been investigated by recording the ionization efficiency curves and measuring the threshold energies for C_2H^- and H^-. For the latter ion the threshold being at 18.0 ±0.1 eV [44], this mechanism of production of C_2H^+ has also to be discarded as responsible for the signal observed below 17.3 eV. They could not be detected by PEPICO.

Finally the second appearance energy of C_2H^+ as determined by electron impact, i.e. at 18.27±0.10 eV in C_2H_2 and at 18.45±0.26 eV in C_2D_2, corresponds remarkably well to the sharp increase in the PIPECO signal at the same energy (see Fig. 6b). This threshold correlates with the adiabatic ionization energy of $C_2H_2^+$. This state is fully predissociated as shown by Fig. 6c by the absence of any $C_2H_2^+$ coincidence signal in the corresponding energy range. To interpret this onset it is likely to assign it to the reaction

$$C_2H_2 + h\nu\,(e^-) \rightarrow C_2H_2^+ (B^2\Sigma_u^+) \xrightarrow[^4\Sigma^-]{\text{prediss}} C_2H^+ (A^3\Sigma^-) + H\,(^2S_g) + (2)e^- \quad (6)$$

where the C_2H^+ ion should be in its first excited $A^3\sum^-$ state at 0.7-1.0 eV above the ground vibronic state [23, 45, 46].

The conclusions drawn from the foregoing discussion have been included in the schematic potential energy diagram along the H-C_2H reaction coordinate shown in Fig. 12.

4.2 The CH^+(CD^+) dissociative ionization channel

The lowest onset energy for CH^+ production is 20.83±0.05 eV, whereas for CD^+ it is measured at 20.61 ±0.07 eV. The electron impact values reported in the literature scatter between 20.0±1.0 eV [47] to 23.1 eV [48]. By photoionization only one determination is reported at 20.7 keV [32]. Initial KE of 50 meV has been measured on CH^+ and no KE is observed on CD^+. The KE versus AE diagram related to CH^+ and CD^+ are shown in Figs. 8 and 9. The straight line (1) and (1') correspond to the lowest energetic process. Both linear regressions are characterized by a correlation coefficient better than 0.99. For CH^+ a slope and extrapolation to KE = 0.0 eV are 0.39±0.02 and 20.85±0.05 eV. For the isotopic counterpart CD^+ the same quantities are 0.35 ±0.01 and 20.47 ±0.02 eV. Though at the limit of the estimated error, the experimental data related to CD^+ are systematically lower than those related to CH^+. This displacement should be significant and have a physical meaning on the base of two arguments: (i) the very good correlation coefficients of straight line (1) (0.994) and (1') (0.999) and (ii) the full overlap of the data of CH^+ and CD^+ giving rise to line (2) in Fig. 9. Any systematic error on the first data set would have led to a comparable error of the same sign on the measurement of the second onset.

The production of CH^+ from C_2H_2 at the thermodynamic threshold should provide the fragments in their ground vibronic state through the reaction

$$C_2H_2 + e^- \rightarrow CH^+ (X^1\Sigma^+, v=0) + CH (X^2\Pi, v=0) + 2e^- \qquad (6)$$

Considering the difference of CH^+ and CD^+ as significant, the lowest onset should be at 20.47±0.02 eV for KE(CD^+) = 0.0 eV. Subtracting the ionization energy (IE(CH) = 10.64 eV (see Table 1) the value *D(DC≡CD)= D(HC≡CH)=9.83±0.10 eV* is obtained. This identity is justified, the error being much larger than the expected isotope effect.

The dissociation energy thus obtained could be compared with earlier values. Thermodynamical calculations [49, 50] agree about a value of 9.97 eV. Ervin *et al.* [16] deduced an energy of 10.00 ±0.03 eV from negative ion photoelectron spectroscopy. Herzberg [13] proposes 9.886 eV as being the most reliable value. Theoretical calculations provide a dissociation energy of 9.826 eV. The present determination of 9.83±0.10 eV fits in this set of values.

The production of ground state fragments should only be valid for CD^+ from C_2D_2 at 20.47 eV. For CH^+ from C_2H_2, the energy difference of 20.83(±0.08)-20.47(±0.02) = 0.36±0.10eV should be ascribed to the vibrational excitation of CH^+ or CH, i.e. $\omega_e(CH^+)$ = 0.339 eV and ω_e(CH) = 0.354 eV [14].

The straight lines (1) and (1') (see Figs. 7 and 8) are characterized by an identical slope of 0.39. This is significantly different from the expected value of 13/26 = 0.500. This is indicative of the partitioning of the excess energy between translational and internal energy carried by the fragments. For both CH^+ and CD^+ an energy balance could be made. Both fragments carry up to 0.5 eV kinetic energy or 1.0 eV in terms of total energy. Subtracting this quantity from the difference (21.90-20.47) eV (see Fig. 8), one obtains an excess energy of 0.4 ±0.1 eV corresponding fairly well to two vibrational quanta of CD^+ or CD, i.e. $\omega_e(CD^+)$ = 0.251 eV and ω_e(CD) = 0.260 eV [14]. Concerning CH^+, likely produced in its ($X^1\Sigma^+$, v = 1) level, the internal energy is estimated in the same way to be 0.25±0.1 eV (see Fig. 7) which could fit only one quantum number of CH^+ or CH [14]. The detailed mechanism describing the production of CH^+ and CD^+ at their lowest onset should be through the reaction

$$C_2H_2(C_2D_2) + e^- \rightarrow C_2H_2(C_2D_2)^* \xrightarrow[\text{ioniz.}]{\text{auto}} [C_2H_2(C_2D_2)]^+(B^2\Sigma_u^+) + 2e^-$$

$$\xrightarrow[X^2\Pi_u]{\text{predis}} CH^+ (X^1\Sigma^+, v=1\rightarrow2) + CH (X^2\Pi, v=0)$$

$$\xrightarrow[X^2\Pi_u]{\text{predis}} CD^+ (X^1\Sigma^+, v=0\rightarrow2) + CD (X^2\Pi, v=0)$$

where the vibrational excitation could be equally transferred to CH(CD). In the above reaction scheme, $^1\Sigma^+$-$^2\Pi$ fragments correlate with a $^2\Pi$ molecular ion state. In the energy range to be considered the $C_2H_2^+$ ($B^2\Sigma_u^+$) state could be populated by autoionization (see Fig. 6a) and is predissociated by the continuum of the $X^2\Pi_u$ state.

Only observed for CD^+, the straight line (1") corresponds to an onset $AE(CD^+)_{KE=0.0}$ = 20.90±0.05 eV, in excellent agreement with the extrapolated value of 20.85±0.05 eV for CH^+. This would be a first argument favouring the assignment

$$C_2D_2 + e^- \rightarrow CD^+ (X^1\Sigma^+, v) + CD (X^2\Pi, v=0) + 2e^-$$

to this threshold. A second experimental evidence supporting this interpretation is the slope on the linear fit (1"), i.e. s^i = 0.224±0.004 with a correlation coefficient of 0.999. The corresponding slope in CH^+ is s = 0.39±0.02. The isotope effect on the vibrational energy can be predicted by determining the ratio $\varrho = (\omega_e^i/\omega_e)^2$ [52] which has been shown to be given by s^i/s [20]. In the present case

$$s^i/s = 0.57 \pm 0.04;\ \varrho^{ion} = 0.54;\ \varrho^{neutral} = 0.55.$$

Though the good agreement between experiment and predictions, it is not allowed to decide whether CD and/or CD^+ are excited. Furthermore, from a simple energy balance in C_2D_2, between 20.9 and 23.2 eV the dissociation process is

$$C_2D_2 + e^- \rightarrow CD^+ (X^1\Sigma^+, v=1,2 \rightarrow 6,7) + CD (X^2\Pi, v=0) + 2e^-$$

Straight line (2) in Figs. 8 and 9 has a slope of 0.52 ±0.02 and extrapolates to KE = 0.0 eV at 21.23±0.04 eV for CH^+ and at 21.18±0.07 eV for CD^+. The most obvious interpretation of this onset would be

$$C_2H_2 + e^- \rightarrow C_2H_2^* \xrightarrow[\text{ioniz.}]{\text{auto}} C_2H_2^+ (B^2\Sigma_u^+) + 2\,e^-$$
$$\xrightarrow[^4\Sigma]{\text{prediss}} CH^+ (X^1\Sigma, v=0) + CH (a^4\Sigma^-, v=0) \qquad (7)$$

where the CH radical is produced in its first electronic excited state at 0.724 eV above the ground state (see Table 1). This spectroscopic value has to be compared with the energy difference of 0.73 ±0.12 eV determined in this work. The total excess energy is converted in translational energy carried by the fragments. This reaction has to run over a C_2H_2 autoionizing state identified at 21.0 eV in the threshold photoelectron spectrum [11]. Autoionization is allowed to the nearest $B^2\Sigma_u^+$ ionization continuum. This state would be predissociated by a $^4\Sigma$ state, the only ionic state correlating with both fragments.

At 21.8±0.1 eV straight line (3) is characterized by a slope of 0.30±0.02 for CH^+ and 0.26±0.02 for CD^+. The energy difference of 21.8(±0.1) - 20.5(±0.08) = 1.3±0.18 eV could be accounted for by the electronic excitation of CH^+ in its $a^3\prod$ state. By optical spectroscopy this energy interval is 1.141 eV (see Table 1). The most straightforward assignment would be the mechanism 8

$$C_2H_2 + e^- \; C_2H_2^*/C_2H_2^+ (C^2\Sigma_g^+) \xrightarrow[^4\Sigma]{\text{prediss}} CH^+ (a^3\Pi) + CH (X^2\Pi) + 2\,e^-. \qquad (8)$$

Both fragments correlate with doublet and quartet Σ and *A* states. On the basis of the usual selection rules and Hund's rule [52] a $^4\Sigma$ would be expected to be involved in (8). Both the Rydberg state at 21.5 eV and the ionic state at 23.5 eV [11, 28, 29] are predissociated.

The same reaction (8) would account for the CH^+ ions observed between 22 eV and 25 eV and for which the data correspond to the straight line (5) extrapolating to 21.8±0.12eV. The same intermediate states are involved. However, the predissociating state would be a $^2\Sigma$ state, lying above the $^4\Sigma$ state, but correlated to the same reaction products.

The above discussed reaction mechanisms have been schematically drawn in a potential energy diagram displayed in Fig. 12 along the HC≡CH reaction coordinate.

The data fitting the straight line (4) give rise to $AE(CH^+)_{KE=0.0}$=22.6 ±0.1 eV and the slope is 0.53 ±0.03. The extrapolation energy is in fairly good agreement with the thermodynamic onset calculated for

$$C_2H_2 + e^- \rightarrow C_2H_2^+ (C_2\Sigma_g^+) \xrightarrow[^2\Pi]{\text{prediss}} CH^+ (a^3\Pi) + CH (a^4\Sigma^-) + 2e^- \quad (9)$$

at 22.35±0.10 eV (see Table 1). The reaction would occur through the $C^2\Sigma_g^+$ hypersurface predissociated by a $^2\Pi$ which correlate with both fragments in their first electronic excited state.

The appearance energies of CH^+ observed above 26 eV are difficult to assign unequivocally to well defined processes. Several mechanisms are predicted to occur in a fairly narrow energy band (data from Table 1). Both CH^+ and CH could be excited to higher electronic states and/or can dissociate. In the energy range of 26-29 eV, X-ray valence-excitation photoelectron spectroscopy shows the existence of a number of dissociative $^2\Sigma$ states [29, 30] likely involved in the dissociative ionization processes considered in this energy range.

Above an energy gap of about 5 eV, up from 34 eV, CH^+ ions are essentially produced with large amounts of translational energy. This energy range corresponds to that of the double ionization energy continuum of C_2H_2. At 33.8 eV the CH^+ ion carries 1.4-3.5 eV kinetic energy. The energy balance with these data leads to $AE(CH^+)_{KE=0.0}$ = 26.8±0.3 eV. This is well below the first double ionization energy of C_2H_2, measured at 32.2 eV [1], and the thermodynamic onset calculated at 31.1 ±0.1 eV for the reaction

$$C_2H_2 + e^- \rightarrow 2CH^+ (X^+\Sigma^+) + 3e^-. \quad (10)$$

Probably an intermediate $C_2H_2^+$* state is involved, lying in the double ionization continuum.

Between 36-42 eV two onsets are measured at 36.2±0.5 eV and at 38.5±0.6 eV respectively. The former threshold is related to the reaction 10 where the products correlate with the only C_2H^{2+} ($^1\Sigma^+$) state. An energy balance on this onset provides $AE(CH^+)_{KE=0.0}$ = 31.4±0.5 eV, in good agreement with the predicted onset for reaction 10 at 31.1 ±0.1 eV. Finally the process at 38.5±0.6 eV could be ascribed to

$$C_2H_2 + e^- \rightarrow CH^+ (X^1\Sigma^+) + CH^+ (a^3\Pi) + 3e^- \quad (11)$$

for which the thermodynamic onset is calculated at 32.24±0.10 eV. No doubly ionized C_2H_2 state has been observed experimentally in this energy range. However, quantum mechanical calculations predict $^3\Pi$ states in this range [53]. These are very likely unstable in the Franck-Condon region.

4.3 The C^+, C_2^+ and CH_2^+ dissociation channels

4.3.1

As shown in Fig. 10, at low electron energy the C^+ ions are produced with small amounts of kinetic energy whereas they carry large translational energies above 26 eV. The lowest threshold of C^+ is measured at 21.16±0.3 eV and is difficult to compare with the broadly scattering values reported in the literature [18, 36, 48]. The first thermodynamical onset is calculated at 20.22±0.10 eV for the reaction

$$C_2H_2 + e^- \rightarrow C^+ (^2P_u) + CH_2 (X^3\Sigma_g^-) + 2e^- \quad (12)$$

which is about 1 eV below the present experimental determination. However, the CH_2 radical is characterized by its a^1A_1 and b^1B_1 states at 0.4 eV and 1.3 eV [13, 54] respectively above its ground state. The suggested reaction mechanism at 21.16 eV is

$$C_2H_2 + e^- \xrightarrow[\text{isomer}]{\text{autonion}} [H_2C{=}C^+, {}^2A_1] \rightarrow C^+ (^2P_u) + CH_2(a^1A_1, v^*) + 2e^- \quad (13)$$

where CH_2 carries internal energy to account for the slope of 0.38 of straight line (1). This reaction has to occur (i) through autoionization of the Rydberg state at 21.5 eV [11] and (ii) over an isomerisation mechanism involving the vinylidene structure of the ion.

The onsets (2) and (3) at 22.4±0.2eV and 23.65±0.13 eV are also defined by a restricted number of data points (see Fig. 10). In both cases the slope of the respective straight lines are significantly lower than the predicted 14/26 = 0.54 value. An excess energy of 22.24-20.22 = 2.02±0.3 eV is measured for (2) and the reaction

$$C_2H_2 + e^- \xrightarrow[\text{isomer}]{C^2\Sigma_g^+} [H_2C{\equiv}C^+] \rightarrow C^+(^2P_u) + CH_2(b^1B_1, v^*) + 2e^- \quad (14)$$

could be invoked for the assignment. It should occur at the expense of the $C_2H_2^+$ ($C^2\Sigma_g^+$) state. The energy difference of 23.65-20.22 = 3.43± 0.23 eV could be accounted for by

$$C_2H_2 + e^- \rightarrow C^+(^2P_u) + C(^3P_g) + H_2(X^1\Sigma_g^+, v^*) + 2e^- \quad (15)$$

calculated at 23.53±0.20 eV and where H_2 carries excess internal energy.

Above 26 eV electron energy onsets are observed at 26.45±0.10 eV, 28.5±0.3 eV and 29.7±0.10eV. By linear regression extrapolations to KE(C^+) = 0.0eV are obtained at 25.38±0.20eV, 27.42±0.20eV and 28.76±0.12 eV respectively. The slope of the straight lines (4)-(7) is 0.38. Consequently, the corresponding processes involve vibrational excitation of a di(poly)atomic fragment. For onsets (4) and (5) the processes could be

$$C_2H_2 + e^- \rightarrow C^+(^2P_u) + H(^2S_g) + CH(a^4\Sigma^-/A^2\Delta, v^*) + 2e^- \quad (16/17)$$

for which the onset is calculated at 25.32±0.20 eV and 27.44±0.20 eV respectively. For the onset detected at 29.7 eV and extrapolating to 28.8 eV, the mechanism (18) should require 28.9 eV comparing satisfactorily with the experimental value of 28.76±0.12 eV

$$C_2H_2 + e^- \rightarrow C^+(^4P_u) + C(^3P_g) + H_2(X^1\Sigma_g^+, v^*) + 2e^-. \quad (18)$$

The fragmentation pattern of C_2H_2 in this energy range does not necessarily involve the vinylidenic structure of $C_2H_2^+$ as a transient. However, as in the previously discussed dissociation channels, the dissociative $^2\Sigma^+$ ionic states detected in the X-ray valence-shell photoelectron spectrum [29, 30] would play an essential role.

4.3.2

The C_2^+ dissociation channel is open at 18.44±0.07 eV. This is in rather good agreement with previous electron impact works [18, 36, 47, 48]. By photoionization [32] the onset is determined at 18.16 eV. The calculation of the thermodynamical onset for C_2^+ production through the reaction (19), i.e.

$$C_2H_2 + e^- \rightarrow C_2H_2^+(B^2\Sigma_u^+) \xrightarrow[\text{prediss}]{\text{isomer}} C_2^+(X^4\Sigma_g^-) + H_2(X^1\Sigma_g^+) + 2e^- \quad (19)$$

involves the value of the H-C_2 binding energy. Using the data of Table 1 and assuming the C_2^+ ion carrying no kinetic energy, a value of *D(H-C_2)=5.44±0.4 eV* is obtained. By other experimental methods 5.20 eV and 5.11 ±0.11 eV are proposed [12, 16, 37]. By theoretical calculations 4.86 eV is obtained [56]. The present electron impact value is very likely overestimated, owing to the shape of the ionization efficiency curve in the threshold region.

The onset of 18.44 eV corresponding very well to the ionization energy of the 2 σ_u orbital, the dissociation mechanism is probably a predissociation of the $C_2H_2^+$ ($B^2\Sigma_u^+$) state (see Fig. 6a). It should occur after isomerisation of the molecular ion into its vinylidenic structure. A $^4B_2$ state, as derived from the $^4\Sigma_g^-$ state, should be the predissociating state.

At 19.58±0.14eV the second C_2^+ threshold is measured. The excess energy of 1.14±0.18 eV has to be ascribed very likely to the electronic excitation of C_2^+ in the $a^2\Pi_u$ or $A^4\Pi_g$ state. These are calculated at 0.82 eV and 1.3 eV above the ground state [57, 58]. The energy level of 19.58 eV still lies in the $B^2\Sigma_u^+$ state energy range, but corresponds to the end of the vibrational structure of this state (see Fig. 6a).

To the threshold at 23.00±0.12 eV corresponds an important increase of the ionization efficiency. The energy difference of 23.00—18.44 = 4.56 ±0.18 eV has very probably to be assigned to the dissociation of H_2 which requires 4.476 eV (see Table 1). At this energy the reaction

$$C_2H_2 + e^- \rightarrow C_2H_2^+(C^2\Sigma_g^+) \xrightarrow[^4\Sigma]{\text{prediss}} C_2^+(X^4\Sigma_g^-) + 2\,H(^1S_g) + 2e^- \quad (20)$$

should take place and its onset energy lies in the energy range of the $C_2H_2^+$ ($C^2\Sigma_g^+$) state which has to be predissociated by a $^4\Sigma$ state correlating with the fragments.

4.3.3

For the reasons already mentioned, the CH_2^+ ion is only investigated below 24.3 eV. The onsets above this level correspond to the N^+ production from N_2 [9].

The first onset for CH_2^+ production is determined at 19.74±0.20 eV (see Fig. 11). The experimental data fit a straight line (1) with a slope of 0.45 ±0.02. It has to be compared to the predicted value of 12/26 = 0.46. The thermodynamical onset for

$$C_2H_2 + e^- \xrightarrow{\text{ioniz}} C_2H_2^+(B^2\Sigma_u^+) \xrightarrow[\text{prediss}]{\text{isomer}} CH_2^+(X^2B_1) + C(^3P_g) + 2e^- \qquad (21)$$

is calculated at 19.36±0.10 eV. The discrepancy between experimental and predicted onset would be ascribed to the slow increase of the ionization efficiency a threshold. Hayaishi *et al.* [32] reported an appearance energy of 19.4 eV. Their photoionization efficiency curve shows a long tailing portion at the onset. Very likely the $C_2H_2^+$ ($B^2\Sigma_u^+$) state is involved in this reaction (see Fig. 6a). This state should isomerize to the vinylidene structure before it predissociates through a $^2A_1$ or a $^2B_2$ state.

The second appearance energy of CH_2^+ is detected at 21.1 ±0.1 eV and corresponds to straight line (2). The energy difference of 21.1-19.4 = 1.4±0.4eV could probably be assigned to the electronic excitation of the C atom in its ^1D_g level at 1.264 eV above the ground level. The CH_2^+ ion producing reaction at this energy should be

$$C_2H_2 + e^- \rightarrow C_2H_2^* \xrightarrow[\text{isomer}]{\text{autoion}} CH_2^+(X^2B_1) + C(^1D_g) + 2e^- \qquad (22)$$

where the Rydberg state at 23 eV participate in this reaction.

Acknowledgments

We are indebted to the Université de Liège, the Fonds National de la Recherche Scientifique (FNRS) and the Fonds de la Recherche Fondamentale Collective (FRFC) for financial support.

References

1. M. Davister and R. Locht, Chem. Phys. 189 (1994) 805 and references therein.

2. R. Locht and J. Schopman, Intern. J. Mass Spectrom. Ion Phys. 15 (1974) 361.

3. Ch. Servais and R. Locht, Intern. J. Mass Spectrom. Ion Processes, to be published.

4. I. Lindau, J. C. Helmer and J. Uebbing, Rev. Sci. Instrum. 44 (1973) 265.

5. A. Lofthus and P. H. Krupenie, J. Phys. Chem. Ref. Data 6 (1977) 113.

6. C. E. Moore, Ionization potentials and ionization limits derived from the analyses of optical spectra, NSRDS-NBS 34 (1970).

7. J. E. Reutt, L. S. Wang, J. E. Pollard, D. J. Trevor, Y. T. Lee and D. A. Shirley, J. Chem. Phys. 84 (1986) 3022.

8. J. N. Miller, Spectrosc. Intern. 3(3) (1991) 42; 3(4) (1991) 41 ; 3(5) (1991) 43.

9. R. Locht, J. Schopman, H. Wankenne and J. Momigny, Chem. Phys. 7 (1975) 393.

10. R. G. Cavell and D. A. Allison, J. Chem. Phys. 69 (1978) 159.

11. R. Locht, K. Hottmann and H. Baumgartel, to be published.

12. R. S. Urdahl, Y. Bao and W. H. Jackson, Chem. Phys. Letters 178 (1991) 425.

13. G. Herzberg, *Molecular spectra and molecular structure. Vol. 3.* Electronic spectra of polyatomic molecules (Van Nostrand, Princeton 1967).

14. K. P. Huber and G. Herzberg, *Molecular spectra and molecular structure. Vol. 4.* Constants of diatomic molecules (Van Nostrand Reinhold, New York 1979).

15. H. Hotop and W. C. Lineberger; J. Phys. Chem. Ref. Data 14 (1985) 731.

16. K. M. Ervin, S. Gronert, S. E. Barlow, M. K. Gilles, A. G. Harrison, V. M. Bierbaum, C. H. DePuy, W. C. Lineberger and G. B. Ellison, J. Am. Chem. Soc. 112 (1990) 5750.

17. C. E. Moore, *Atomic energy levels. Vol. 1.* NSRDS-NBS Circ. 467 (USGPO, Washington D.C. 1949).

18. P. Kusch, A. Hustrulid and J. T. Tate, Phys. Rev. 52 (1937) 843.

19. H. Shiromura, Y. Achiba, K. Kimura and Y. T. Lee, J. Phys. Chem. 91 (1987) 17.

20. R. Locht, J. L. Olivier and J. Momigny, Chem. Phys. 43 (1979) 425.

21. S. Shih, S. D. Peyerimhoff and R. J. Buenker, J. Mol. Spectrosc. 64 (1977) 167.

22. S. Shih and S. D. Peyerimhoff, J. Mol. Spectrosc. 74 (1979) 124.

23. A. G. Koures and L. B. Harding, J. Phys. Chem. 95 (1991) 1035.

24. P. G. Carrick, A. J. Merer and R. F. Curl Jr., J. Chem. Phys. 78 (1983) 3652.

25. R. F. Curl Jr., P. G. Carrick and A. J. Merer, J. Chem. Phys. 83 (1985) 4278.

26. E. Somè, F. Remy, D. Macau-Hercot, I. Dubois, J. Breton and H. Bredohl, accepted in J. Mol. Spectrosc. (1995).

27. W. R. Graham, K. I. Dismuke and W. Weltner, J. Chem. Phys. 60 (1974) 3817.

28. G. Bieri and L. Åsbrink, J. Electron. Spectrosc. Relat. Phenom. 20 (1980) 149.

29. S. Svensson, E. Zdansky, U. Gelius and H. Ågren, Phys. Rev. A37 (1988) 4730.

30. J. Muller, R. Arneberg, H. Ågren, R. Manne, P. Å. Mannquist, S. Svensson and U. Gelius, J. Chem. Phys. 77 (1982) 4895.

31. S. R. Andrews, F. M. Harris and D. E. Parry, Chem. Phys. 166 (1992) 69.

32. T. Hayaishi, S. Iwata, M. Sasanuma, E. Ishiguro, Y. Morioka, Y. Iida and M. Nakamu-ra, J. Phys. B15 (1982) 79.

33. Y. Ono and C. Y Ng, J. Chem. Phys. 74 (1981) 6985.

34. K. M. Weitzel, J. Mähnert and M. Penno, Chem. Phys. Letters 224 (1994) 371.

35. K. Norwood and C. Y. Ng, J. Chem. Phys. 91 (1989) 2898.

36. P. Plessis and P. Marmet, Int. J. Mass Spectrom. Ion Processes 70 (1986) 23.

37. J. R. Wyatt and F. E. Stafford, J. Phys. Chem. 76 (1972) 1913.

38. B. K. Janousek and J. I. Braunian, J. Chem. Phys. 71 (1979) 2057.

39. M. Iraqi, A. Petrank, M. Peres and C. Lifshitz, Int. J. Mass Spectrom. Ion Processes 100 (1990) 679.

40. I. Dotan, M. Iraqi and C. Lifshitz, Int. J. Mass Spectrom. Ion Processes 124 (1993) R21.

41. P. G. Green, J. L. Kinsey and R. W. Field, J. Chem. Phys. 91 (1989) 5160.

42. Y. Chen, D. M. Jonas, C. E. Hamilton, P. G. Green, J. L. Kinsey and R. W. Field, Ber. Bunsenges. Phys. Chem. 92 (1983) 329.

43. M. Fuji, A. Haijima and M. Ito, Chem. Phys. Letters 150 (1988) 380.

44. R. Locht and J. Momigny, Chem. Phys. Letters 6 (1970) 273.

45. A. O'Keefe, R. Derai and M. T. Bowers, Chem. Phys. 91 (1984) 161.

46. W. Koch and G. Frenking, J. Chem. Phys. 93 (1990) 8021.

47. G. Cooper, T. Ibuki, Y. Iida and C. E. Brion, Chem. Phys. 125 (1988) 307.

48. J. Momigny and E. Derouane, Adv. Mass Spectrom. 4 (1967) 607.

49. S. W. Benson, J. Chem. Educat. 42 (1965) 502.

50. T. L. Cottrell, *The strength of chemical bonds* (Butterworth, 1958).

51. S. R. Langhoff, C. W. Bauschlicher and P. R. Taylor, Chem. Phys. Letters 180 (1991) 88.

52. G. Herzberg, *Molecular spectra and molecular structure. Vol. 2.* Spectra of diatomic molecules. (Von Nostrand, Princeton 1967).

53. R. Thissen, Ph. D. Thesis, Université de Liège (1992).

54. I. Shavitt, Tetrahedron 41 (1985) 1531.

55. P. Rosmus, P. Botschwina and J. P. Maier, Chem. Phys. Letters 84 (1981) 71.

56. C. W. Bauschlicher and S. R. Langhoff, Chem. Phys. Letters 173 (1990) 367.

57. C. Petrongolo, P. G. Bruna, S. D. Peyerimhoff and R. J. Buenker, J. Chem. Phys. 74 (1981) 4594.

58. P. Rosmus, H. J. Werner, E. A. Reinsch and M. Larsson, J. Electron Spectrosc. Relat. Phenom. 41 (1986) 289.